THE JOURNAL OF PHYSICAL CHEMISTRY B

Article

pubs.acs.org/JPCB

Conformational Distributions and Hydrogen Bonding in Gel and Frozen Lipid Bilayers: A High Frequency Spin-Label ESR Study

Boris Dzikovski, Dmitriy Tipikin, and Jack Freed*

National Biomedical Center for Advanced ESR Technology (ACERT), Department of Chemistry and Chemical Biology, Baker Laboratory, Cornell University, Ithaca, New York 14853, United States

Supporting Information

ABSTRACT: The ESR parameters of PC spin labels in frozen membranes do not simply represent the membrane polarity or water penetration profile. Instead, they show a distribution between hydrogen-bonded (HB) and non-hydrogen-bonded (non-HB) states, which is affected by a number of factors in the membrane composition. Similar to the exclusion of solutes from crystallizing solvents, the pure bulk gel phase excludes nitroxides, forcing acyl chains to take bent conformations. In these conformations, the nitroxide is hydrogen-bonded. Furthermore, upon gradual cooling in the supercooled gel, PC labels undergo slow lateral aggregation, resulting in a broad background signal. However, if the sample is instantly frozen, this background is replaced by the HB component. In membranes with cholesterol, the observed HB/non-HB ratio can best be described by a partition-like equilibrium between nitroxides located in defects of lipid structure within the hydrophobic core and those close to the membrane surface.

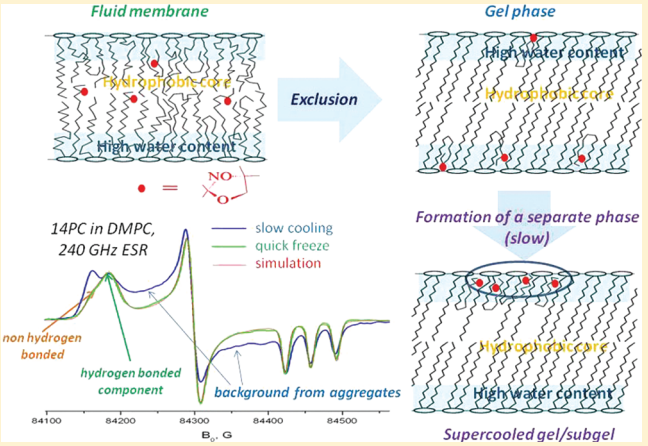

INTRODUCTION

Lipid spin labels containing nitroxide groups at different positions in the fatty acid chain, such as 1-palmitoyl-2-stearoyl-(*n*-doxyl)-*sn*-glycero-3-phosphocholines (*n*-PC spin labels), are a useful and proven tool in lipid research. Through a vast number of studies, they have provided crucial insights into the structure of model and biological membranes, reported on the membrane fluidity, polarity, phase state, and presence of microscopic domains,[1] accessibility of different depth positions in the lipid bilayer for oxygen and other polar and nonpolar paramagnetic compounds.[2−4] PC spin labels have also provided valuable information on protein/lipid interactions and boundary lipids.[5,6]

It is generally accepted that, unlike bulky fluorescent labels,[7,8] nitroxides are well incorporated into fluid lipid bilayers[9] and not excluded from them. However, it has been shown by NMR that, although the most probable location of the nitroxide group for 5-, 10-, and 16-PC spin labels in the fluid POPC membrane corresponds to the fully extended conformation, the distribution is relatively broad and other conformations should also be present.[10] Bent conformations were previously found for doxylstearic acids in monomolecular films,[11] water/hydrocarbon emulsion particles,[12] and micellar systems.[13] In fluid membranes, the fluidity, polarity, and accessibility parameters reported by ESR using PC spin labels and *n*-doxylstearic acids are, in general, in good agreement with the extended conformation of the spin-labeled alkyl chain and change monotonically with an increase in *n*,[3,14] although there are indications that the spin-label groups on the stearates are located nearer to the membrane exterior than the analogous positions of the unlabeled phospholipid chains.[15] However, in the gel phase, which is characterized by denser chain packing and higher order, the behavior and location of nitroxides may differ. Although most cell membranes in vivo exist in the fluid L_α phase, the gel phase of lipid bilayers has biological interest for specialized membranes such as stratum corneum[16,17] or lens.[18]

ESR spectroscopy and high field ESR, in particular, have been used at low temperatures to determine polarity profiles in membranes of various compositions: Earle et al.[19] at 250 GHz, Kurad et al., Subczynski et al.[20,21] at 94 GHz. In these studies, the polarity of the local environment was monitored by *g*-tensor and hyperfine splitting values. However, some observations on the behavior of PC spin labels and features of their ESR spectra are yet to be completely understood. For example, high field ESR, which is very sensitive to local polarity and proticity,[22] in DMPC/cholesterol membranes containing *n*-PC labels at 94 GHz shows the presence of two components with different g_{xx} values.[21,14] Although these components cannot be completely

Special Issue: Harold A. Scheraga Festschrift

Received: December 9, 2011
Revised: February 9, 2012
Published: February 13, 2012

   dx.doi.org/10.1021/jp211879s | *J. Phys. Chem. B* 2012, 116, 6694−6706

resolved at W-band (94 GHz), the more polar component (lower g_{xx}) is clearly detectable for n values higher than 7 on the background of the component with a higher g_{xx} value. The superior g-factor resolution, which is provided by a 170/240 GHz quasioptical spectrometer available at ACERT was expected to completely resolve and identify these components. Also, while all PC spin labels in DPPC containing gramicidin A were characterized at low temperatures by well resolved high field rigid limit spectra,[19] 7-, 10-, and 12-PC in pure DPPC show a singlet-like background signal as the major spectral component. This background signal, however, is much less pronounced in cholesterol-containing membranes, even with low cholesterol content.[21] This difference could be attributed to a specific behavior of PC spin labels in the L'_β phase of pure phospholipids. This densely packed phase (tilted gel phase) could behave as a two-dimensional analogue for a bulk fluid phase which upon freezing and crystallization excludes dissolved spin labels into high concentration areas with strong spin−spin interactions. Addition of a third component like GA[19] or cholesterol[21] for this case can perturb the lipid chain packing and provide more defects to incorporate and spatially separate the nitroxide rings.

The purpose of the current study is to better understand how spin-labeled molecules report on the lipid polymorphic phases, in particular the gel phase, to explain previously observed aggregation patterns and their connection to the membrane phase state and composition. This work illustrates superior resolution of HF ESR, its advantages in membrane studies, and benefits of simultaneous application of several ESR techniques; it also points at the conformational flexibility of PC spin labels, which should be taken into account in all studies where they are used.

MATERIALS AND METHODS

Materials. Spin-labeled phosphatidylcholines, *n*-PCSL (1-acyl-2-[*n*-(4,4-dimethyloxazolidine-*N*-oxyl)stearoyl]-*sn*-glycero-3-phosphocholine) with n = 5, 7, 10, 12, 14, or 16, were purchased from Avanti Polar Lipids and, if necessary, additionally purified using preparative TLC. Synthetic phosphatidylcholines, DMPC (1,2-dimyristoyl-*sn*-glycero-3-phosphocholine), DPPC (1,2-palmitoyl-*sn*-glycero-3-phosphocholine), and egg yolk PC were from Avanti Polar Lipids (Alabaster, AL). 3-Carboxy-2,2,5,5-tetramethylpyrrolidine-1-oxyl was from Acros Organics. Cholesterol, organic solvents, and other chemicals including TEMPO nitroxides were from Sigma-Aldrich.

Preparation of Membrane Samples. Spin-labeled phosphatidylcholines were incorporated in bilayer membranes at a relative concentration of 0.5 mol % by drying down the lipid solutions in chloroform/methanol and then suspending the dry lipid in water above the chain melt temperature for ∼20 min. The suspension was spun down in an Eppendorf tube and supernatant removed. For high field ESR measurements, about 8 μL of the lipid pellet containing ∼2 mg of the lipid was placed between a flat quartz coverslip and an etched quartz coverslip with a circular concavity in the middle. The diameter of the concavity to hold the sample is about 10 mm, and the diameter of the coverslips is 18 mm. A thin layer of vacuum grease (Dow Corning) was applied on the edge to create a seal between the two coverslips. Such a sample holder was discussed in detail elsewhere.[23,24]

For X-band CW saturation measurements, the lipid pellets were resuspended in ∼40 μL of water and transferred into 50 μL, 0.7 mm i.d. glass capillaries and spun down for 10 min at 10000*g* using a microhematocrit centrifuge. The excess water was removed; sample sizes were trimmed to 5 mm length to avoid inhomogeneities in H_1 and H_m fields.[25] To remove oxygen from the lipid and ensure anaerobic conditions in the final ESR samples, the samples in the capillaries were frozen in liquid nitrogen, briefly evacuated using an oil pump, and thawed in the atmosphere of high purity argon. After repeating this procedure three times, the capillaries were flame-sealed under a vacuum with the sample part submerged in liquid nitrogen.

X-Band ESR Spectroscopy. ESR spectra were obtained on a Bruker EMX spectrometer (Bruker, Billerica, MA) at a frequency of 9.55 GHz under standard conditions. The field sweeps were calibrated with a Bruker ER 035 Gmeter. The microwave frequency was monitored with a frequency counter. The temperature was stabilized and monitored by a nitrogen gas flow temperature unit (±0.2 °C accuracy) or, for 77 K measurements, using a finger dewar filled with liquid nitrogen.

For CW saturation experiments, sample capillaries were positioned along the symmetry axis of the standard 4 mm quartz EPR sample tube that contained dodecane for thermal stability. The root-mean-square microwave magnetic field $\langle H_1^2\rangle^{1/2}$ at the sample was measured as described by refs 26 and 25, and corrections were made for the cavity Q value as described in the same reference. The ESR spectra were recorded at a modulation frequency of 100 kHz; the modulation field measured at the sample was 0.32 G p-p.

The dependence on the microwave field for the amplitude of the central component of the EPR spectra was measured and fitted to the equation

$$I = \frac{I_0 \cdot H_1}{(1 + P \cdot H_1^2)^{3/2}} \quad (1)$$

from which the saturation parameter P was obtained. Here, I_0 is the $I-H_0$ slope at low power, where the dependence can be considered linear.

The parameter $\Delta(1/P) = 1/P - 1/P_0$, where P_0 is the saturation parameter in the absence of paramagnetic relaxant, was used as an experimental parameter of relaxation enhancement.

For relaxation enhancement studies by paramagnetic ions present in the water phase of the membrane, we used nickel perchlorate (10 mM), which is shown to be the strongest relaxant among nickel salts for PC spin labels in DMPC and EYL membranes.[27]

High Field ESR. High-field ESR spectra were recorded on a 170/240 GHz (6−9 T) ESR spectrometer, which was designed and built at ACERT at Cornell University.[28] The data collection routine is based on LabView virtual instrument drivers written at ACERT. A Lakeshore 340 temperature controller was used to stabilize the temperature at 80−82 K. It corresponds to the rigid-limit conditions, as evidenced by experiments showing no change in the ESR line shape between this temperature and 100−110 K. MATLAB procedures based on the EasySpin software package[29] were used for simulations of high field ESR spectra at the rigid-limit condition.

Sample Freezing Procedures for High Field ESR. Typically, a low temperature high field ESR experiment uses a helium or nitrogen cryostat. For our experimental setup, it usually takes ∼2+ h to reach the target temperature, with an initial drop from ambient temperature to ∼260 K taking ∼30

dx.doi.org/10.1021/jp211879s | J. Phys. Chem. B 2012, 116, 6694−6706

min. During this cooling process, the lipid bilayer, as discussed below, may pass through a number of slow forming metastable phases. The lateral distribution of lipids and spin labels in these phases may differ from the initial gel phases. Alternatively, to prevent any slow lateral redistribution of lipids during this slow cooling procedure, and to trap the initial distribution, a quick freeze–quench was performed by submerging the whole Fabry–Perot resonator assembly into liquid nitrogen. The cooling rate obtained in this procedure was monitored in test experiments by a temperature-dependent resistance Wheatstone bridge with a 15 Ω thin test tungsten wire placed inside the etched cavity of a standard sample holder for HFHF ESR. The resistance vs time curves were recorded on the oscilloscope using a Stanford Instruments lock-in amplifier. Analysis of these curves shows an initial slope of ~140 K/s; this corresponds to reaching 260 K within 0.2 s. The same immersion procedure with liquid helium instead of liquid nitrogen gives a substantially slower cooling rate of ~40 K/s. After freezing in liquid nitrogen, the Fabry–Perot resonator assembly was quickly inserted into the bore of the magnet, which was precooled by the nitrogen flow cryostat to ~120 K. The cryostat was further used to stabilize the temperature at the target temperature.

Before the freeze–quench procedure, samples of both spin-labeled DMPC and DPPC were kept at room temperature, 292–295 K, for at least 1 h. This temperature is below the main transition for DMPC (297 K), which stays in the P_β rippled gel phase under these conditions. On the other hand, DPPC at this temperature exists in the L'_β phase, which becomes metastable and slowly transforms to the subgel phase only below 280 K.[30]

RESULTS AND DISCUSSION

9 GHz ESR. Table 1 shows the values of the ^{14}N hyperfine constant ($2A_{zz}$) determined by X-band ESR as the outer

Table 1. Hyperfine Splitting Parameter $2A_{zz}$ in DMPC and DPPC Membranes with and without Cholesterol Determined by X-Band ESR at 77 K[a]

	DMPC	DMPC/Chol	DPPC	DPPC/Chol
5	68.9	69.7	69.2	70.1
7	69.3	70.1	69.9 (broadening)	69.1
10	69.6	66.6	69.5 (more broadening)	66.5
12	68.4	66.3	67.2	66.4
14	69.3	66.4	66.3	66.8
16	69.3	66.2	66.7	66.5

[a]To record the ESR spectra, the samples in 1.2 mm ID capillaries after long exposure at 19 °C were quickly submerged into liquid nitrogen.

splitting of the rigid limit spectra at 77 K. As seen from the data, DMPC/cholesterol (cf. Figure S1A, Supporting Information) and DPPC/cholesterol (cf. Figure S1C, Supporting Information) membranes, consistent with previous observations,[3] show an abrupt drop in the polarity, as monitored by the $2A_{zz}$ value, between *n*-PC positions 7 and 10. However, for DMPC, in the absence of cholesterol, the $2A_{zz}$ value shows little trend throughout the PC spin labels series and remains ~69.5 G (cf. Figure 1), which corresponds to a relatively polar environment, more polar than ethanol (see below). DPPC in the absence of cholesterol (cf. Figure S1B, Supporting Information), in general, shows a profile similar to a cholesterol-containing membrane, though the spectra, especially for positions 7–12,

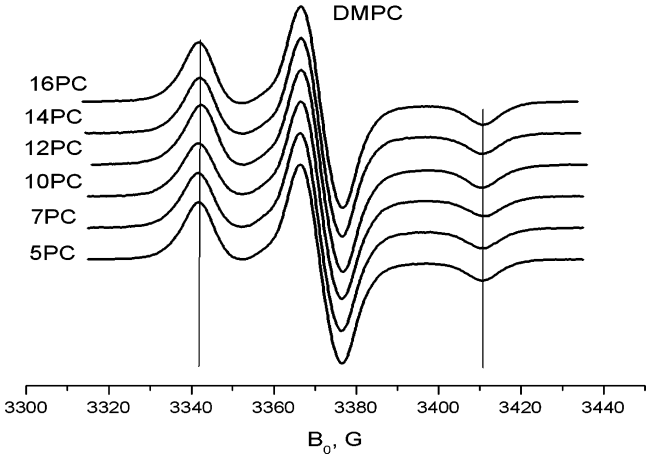

Figure 1. PC spin labels in DMPC at 77 K. The apparent value of $2A_{zz}$ does not change in the PC series.

show signs of a broad singlet-like component (Figure 1C, Supporting Information).

The dependence of relaxation enhancement $\Delta(1/P)$ by 10 mM $Ni(ClO_4)_2$ on the spin-labeling position for the gel and liquid crystal phase of DMPC is given in Figure 2. In the liquid

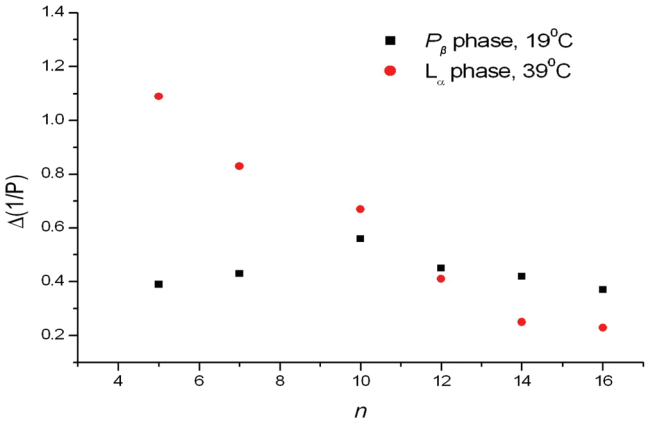

Figure 2. Relaxation enhancement from 10 mM of $Ni(ClO_4)_2$ introduced into the water phase of lipid DMPC dispersions as a function of *n* at the P_β (19 °C) and L_α (39 °C). An almost flat accessibility profile in the gel might indicate similar average membrane immersion depth for the nitroxide moieties of all studied PC labels.

crystal phase (T = 39 °C), the interaction with the paramagnetic relaxant decreases with increasing *n*, consistent with an increase in the average immersion depth of the spin-label moiety in the membrane. On the contrary, the $\Delta(1/P)$ profile in the gel phase (P_β, T = 19 °C) is almost flat (with a minor spike at position 10).

High Field/High Frequency ESR. High frequency ESR and PC spin labels were successfully used to study polarity profiles in phospholipid membranes.[14,19,21] For example, in a detailed ESR study at 250 GHz, 5-, 7-, 10-, 12-, 14-, and 16-PC were studied in DPPC and DPPC/gramicidin systems.[19] It was found that in pure DPPC most spins are strongly aggregated and the spectrum consists mostly (especially for 7–12 PCs) of a singlet-like signal. Although the g-factor values for the resolved rigid-limit component clearly show increasing immersion of the nitroxide into the hydrophobic core of the membrane with increasing *n*, it is difficult to obtain any

dx.doi.org/10.1021/jp211879s | J. Phys. Chem. B 2012, 116, 6694–6706

Table 2. Values of Isotropic Hyperfine Splitting Constant a_{iso} and $2A_{zz}$ Determined at X-Band at 295 and 77 K, Respectively, for Several Solvents[a]

solvent, dielectric constant at room temperature[68]	oxo-TEMPO	TEMPO	4-hydroxy TEMPO	3-carboxy-2,2,5,5 tetramethylpyrrolidine-1-oxyl
isopentane, 1.8	14.27/[b]	15.29/68.2	15.15/[b]	13.92/[b]
MCH, 2.02	14.315/[b]	15.32/68.2	15.20/[b]	13.96/[b]
toluene, 2.4	14.49/67.6	15.53/69.3	15.43/69.1	14.22/66.7
DBPh, 6.4	14.61/67.6	15.64/69.4	15.55/69.2	14.37/66.9
ethanol, 24.3	15.06/70.0	16.21/72.9	16.05/71.0	15.02/70.1
TFE, 26.14	15.63/73.5	17.00/79.7	16.73/77.3	15.77/74.4
water/glycerol, 80.4	15.97/73.8	17.19/76.5	16.96/75.5	16.12/73.2

[a]These A_{zz} values were also used to obtain the best fits for the corresponding 240 GHz rigid limit spectra. [b]The $2A_{zz}$ value at 77 K cannot be reliably determined due to the presence of a singlet-like background.

Table 3. g_{xx} Component of the g-Tensor Determined by 240 GHz ESR at 80−85 K in Several Glass Forming Solvents[a]

solvent, dielectric constant	oxo-TEMPO	TEMPO	4-hydroxy TEMPO	3-carboxy-2,2,5,5 tetramethylpyrrolidine-1-oxyl
toluene	2.009438			
DBPH	2.009445	2.010103	2.010129	2.009230
ethanol	2.009485/**2.008838**	sh/2.009411	2.010040/**2.009456**	2.009250/**2.008533**
TFE	**2.008793**/sh	2.008669	2.009460/**2.009089**	2.008487/sh
water/glycerol	**2.008784**/~2.00850	2.008805	2.009460/**2.008951**	2.008532/sh

[a]A common value of 2.00233 was assigned as g_{zz} for all spin labels, and the g_{xx} value was accurately determined relative to this g_{zz} value from the corresponding spectral splitting.[46,47] If two components are present in the spectrum, the component with higher fraction is marked bold. "Sh" denotes the presence of a high/low field component, which manifests itself not as a distinct peak but as a shoulder on the main component.

information on the location of aggregates which manifest themselves in the broad component. Several W-band (94 GHz) studies by Marsh and co-workers[21,31,14] on DMPC/cholesterol membranes utilized all *n*-PC spin labels in the 4−16 range (except 15-PC). They allowed, based on the g_{xx} values, for obtaining detailed polarity profiles in these systems.

Resolution of Different Hydrogen-Bond States by 240 GHz HFHF ESR in Bulk Organic Solvents. It has been well established that the g-tensor and hyperfine components of nitroxide radicals are very sensitive to the local environment, to polarity and proticity in particular. In general, changing the local environment of the nitroxide moiety from water (polar) to hydrocarbon (nonpolar) causes an increase in the g-tensor components and a concomitant decrease in the values of the components of the hyperfine tensor. This effect is most pronounced for the tensor components g_{xx} and A_{zz}. For example, for the PDT (4-oxo-2,2,6,6-tetramethylpiperidine-d_{16}-1-oxyl) probe in the polar glycerol/water solvent vs toluene, g_{xx} changed by ~0.001,[32] while A_{zz} decreased. In the 1980s, Lebedev and co-workers extensively studied the effects of solvent polarity and demonstrated a high degree of correlation between the values of A_{zz} and g_{xx}.[33] However, the separation of the polarity and proticity effects could complicate the analysis of the ESR spectra. Proticity refers to the propensity to donate hydrogen bonds, whereas aprotic refers to solvents which cannot donate a hydrogen bond. At relatively low frequencies, up to 95 GHz, the separation of hydrogen-bonded vs non-hydrogen-bonded states of the nitroxide often relied upon different g versus A plots, discovered for these two states.[34] However, as shown in a recent study using TEMPO, if the correlations are indeed different for TEMPO in protic and aprotic solvents, the difference is rather small.[35]

On the other hand, superior g-factor resolution of very high-field ESR allows for observation of two resolved spectral components corresponding to two (Smirnova et al.[36] at 130 GHz) or possibly more (Bordignon et al.[37] at 95, 275, and 360 GHz) states of hydrogen bonding. Two hydrogen bonding states coexisting in frozen deuterated alcohols were previously demonstrated for perdeuterated TEMPONE by X-band ESR.[38]

Tables 2 and 3 show the values of A_{zz} and a_{iso} hyperfine splitting and the g_{xx} component of the g-tensor for several nitroxide radicals.

As one sees from Figure 3 and Figure 3S (Supporting Information), whereas at the X-band one sees a continuous increase in the ^{14}N hyperfine splitting with change of the local environment from nonpolar/aprotic to polar/protic, the 240 GHz ESR shows three distinct values of the g_{xx} parameter. Although the presence/ratio of these components strongly

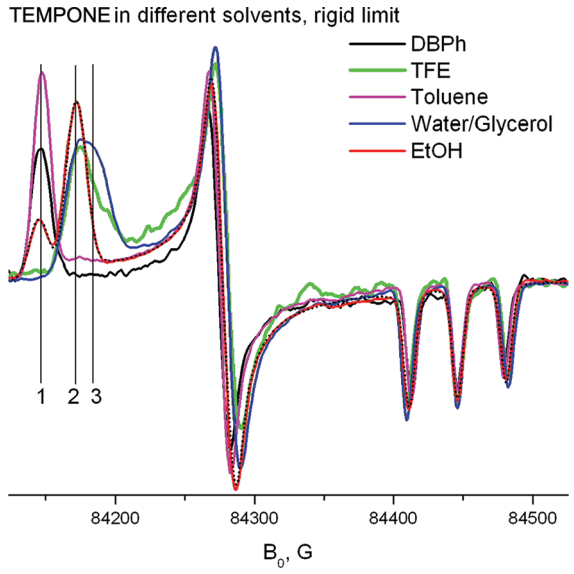

Figure 3. 240 GHz spectra of 4-oxo-TEMPO (TEMPONE) in a series of glass-forming solvents at 80−85 K. The black dotted line is a two-component rigid simulation of the ethanol spectrum. g values 2.009450, 2.008830, and 2.008500 are noted "1", "2", and "3", respectively.

dx.doi.org/10.1021/jp211879s | J. Phys. Chem. B 2012, 116, 6694−6706

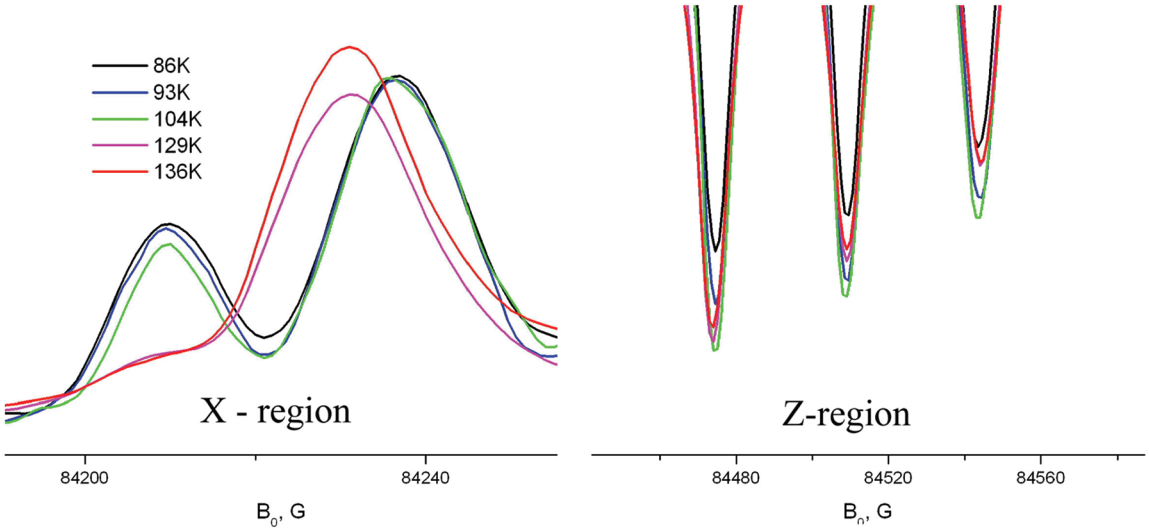

Figure 4. Disappearance of the two-component feature in the X-region of the TEMPONE/ethanol spectrum above 120 K. High field ESR can reliably attribute this effect to the shortening of the hydrogen bond lifetime.

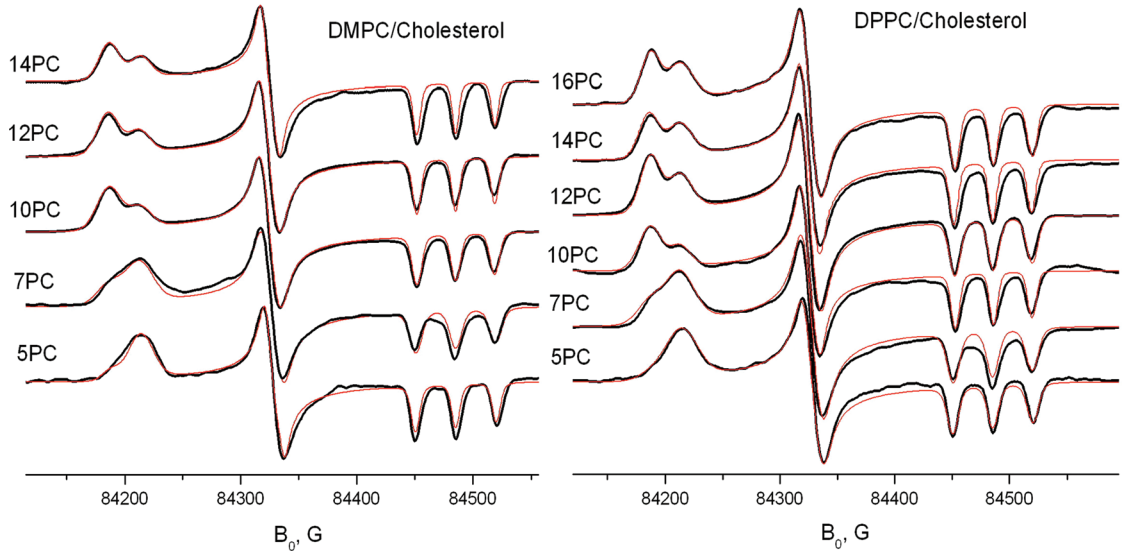

Figure 5. Rigid-limit 240 GHz ESR spectra of *n*-PC spin labels in DMPC and in DPPC containing 30% mol cholesterol. T = 80−82 K. The samples are gradually frozen in the flow of gaseous nitrogen. Red lines show simulations of these spectra using two components with g_{xx} = 2.009435 ± 0.000005 and 2.008820 ± 0.000005 for all spectra. g_{yy} and g_{zz} are taken as 2.006100 and 2.00233 for both components.

depends on the polarity−proticity of the solvent, there is little variation in the g_{xx} measured for each such component. For all four spin labels studied, three distinct components could be detected: (1) "non-polar", as in toluene, DBPh or the minor component in alcohols, (2) "polar", the major component for ethanol and major or minor component in TFE and water/glycerol, depending on the nitroxide used, and (3) "very polar" component observable in TFE and water/glycerol. Although components 2 and 3 cannot be separated at 240 GHz as two distinct peaks, their presence is quite obvious (compare Figure 3 and Figure 3S (Supporting Information) for TEMPOL and TEMPO). We assign these components to different hydrogen-bonding states of nitroxide radicals and speculate that state 2 corresponds to a single hydrogen bond, while state 3 is double-bonded. Existence of multiple hydrogen bonds to a nitroxide has been predicted theoretically[39−41] and later suggested as an explanation for complex ESR lineshapes observed in spin-labeled proteins.[37] Interestingly, the g_{xx} value of the non-hydrogen-bonded component for all four spin labels studied shows little dependence on the polarity of the frozen glass-forming solvent (Table 3). This contrasts with the conspicuous dependence of the hyperfine splitting for nonprotic solvents at room temperature on the dielectric constant ε (cf. Table 2). For protic solvents at 77 K, the resolution at the X-band is insufficient for resolving hydrogen-bonded and non-hydrogen-bonded spectra. However, the hyperfine splitting, a_{iso} at room temperature for aprotic solvents, shows a clear dependence on ε. Also, theoretical predictions for the g-factor,[42] as well as some room temperature measurements for g_{iso}, point to a higher g-factor for lower ε.[34,35]

It is well-known that at room temperature the lifetime of a hydrogen bond is very short and measured on the picosecond time scale.[43] Existence of two distinct spectral states in alcohols at liquid nitrogen temperatures shows that at these conditions the lifetime of the hydrogen bond is long on the time scale of ESR at this frequency and should be longer than ∼100 ns.

dx.doi.org/10.1021/jp211879s | J. Phys. Chem. B 2012, 116, 6694−6706

However, if the ethanol solution containing TEMPONE warms up above ~115 K, some signs of exchange between the components appear: they broaden and start to move toward each other. Eventually, at ~140 K, the low field component of the doublet disappears (Figure 4). High field ESR can reliably attribute this effect to exchange between the hydrogen-bonded and nonbonded states of the nitroxide because of shortening of the hydrogen bond lifetime rather than to motional effects in the ethanol glass (melting point 159 K). Indeed, as seen in Figure 4, the broadening affects only the X-region of the spectrum and leaves the triplet in the Z-region intact. To attribute this spectral change to molecular motion, one would have to assume extremely high-axial Z-rotation, i.e., motion about the axis perpendicular to the nitroxide ring. This is highly unlikely for a relatively spherical molecule like TEMPONE in an isotropic glassy medium.[44]

At this point, we would like to call attention to the superior orientational resolution of high field ESR:[45,46] this conclusion could not be drawn from ESR at low frequencies.

PC Spin Labels in DMPC and DPPC in the Presence of Cholesterol. The polarity profiles previously obtained by HFHF ESR[14] appeared to be almost identical to the polarity profiles previously obtained by rigid limit X-band ESR from the hyperfine splitting[3] values. However, a close inspection of the spectra of ref 21 shows two components, which correspond to hydrogen-bonded and non-hydrogen-bonded states of the nitroxide radical states 2 and 1 (as marked in Figure 3). These two components are discernible not only for the area of abrupt "polarity change" (PC 5−10) but also for PC 14−16. With the higher resolution of 240 GHz ESR, we expected to better separate and identify these components. Figure 5 shows the spectra for DMPC and DPPC in the presence of cholesterol. The ESR spectra in the two different lipids are very similar, nearly identical. There are two components discernible for $n \geq 7$, which are completely resolved for $n \geq 10$, with g_{xx} = 2.009435 and g_{xx} = 2.008820 (with g_{zz} taken as 2.00233, see ref 47). The two g values are nearly the same for all n. For 5-PC, only the polar component is present. While at 94 GHz and even at 170 GHz these components could not be completely separated, see Kurad et al.[21] and our 170 GHz data (not shown), 240 GHz appears as a good frequency to observe them as separate discernible peaks.

It has previously been assumed that the polarity profile reported by spin labels for fluid and frozen membranes containing cholesterol in general follows the membrane water penetration profile.[40,48,49] However, the exact features of the ESR spectrum may be defined by interplay of this water penetration and the flexibility of spin-labeled lipid chains; see below. While the short acyl tether for the nitroxide of 5-PC is always located in the area with higher water content and shows only a hydrogen-bonded component, longer acyl tethers can reach a less polar area with lower water content. However, even for 14- and 16-PC, there is a substantial fraction of hydrogen-bonded component. Moreover, the fraction of the hydrogen-bonded component does not decrease monotonically with an increase in the n number. As seen in Figure 5 and Table 4, this fraction experiences a dramatic drop between 7- and 10-PC and then gradually increases further for positions 12, 14, and 16. On the basis of these observations and what is currently known about flexibility of spin-labeled lipids,[10] we believe that the hydrogen-bonded component mainly corresponds to bent conformations of the spin-labeled lipid chain, rather than penetration of water molecules to the middle of the membrane

Table 4. Ratio of Hydrogen-Bonded, HB (g_{xx} = 2.00882), and Non-Hydrogen-Bonded Components, non-HB (g_{xx} = 2.009435), Determined from Rigid-Limit Simulations of *n*-PC Spin Labels in DMPC and DPPC Containing 30% mol Cholesterol

PC label	ratio HB/non-HB in DMPC	ratio HB/non-HB in DPPC
5	~6	>8
7	1.8	2.3
10	0.32	0.36
12	0.45	0.62
14	0.55	0.8
16		0.8

and forming a hydrogen bond with the nitroxide moiety of the PC spin label in a fully extended conformation.

Indeed, theoretical estimates[50] show that the concentration of water in the middle of the DPPC membrane is ~1 mM. It should be even lower for membranes containing cholesterol, since cholesterol is known to substantially decrease water permeability across lipid membranes.[51,52] For the equilibrium constant between hydrogen-bonded/unbonded forms of 16-sasl in toluene−trifluoroethanol mixtures, Marsh[48] gives a value of ~1 M^{-1}. This value is determined from the isotropic hyperfine splitting at room temperature. Our estimates for this constant based on measurement of $2A_{zz}$ values for TEMPONE and TEMPO in ethanol−DBPH mixtures by 9 GHz ESR quickly frozen at 77 K give values of the same order, 0.5 and 0.3 M^{-1}, respectively (see Figure 4S, Supporting Information). As seen from Figure 3, a two-component rigid-limit simulation for TEMPONE in pure ethanol (~17 M hydroxyl concentration) gives their ratio of 1:3.6 and, hence, a rough estimate of 0.2 M^{-1} for the hydrogen bonding constant. A similar procedure for the 3-carboxy-2,2,5,5 tetramethylpyrrolidine spin-label (Figure 3C, Supporting Information), which is structurally more similar to the nitroxide moiety on PC labels and shows very similar magnetic parameters, gives the component ratio 1:6 and hence a hydrogen bonding constant of ~0.35 M^{-1}. A 1:1 ratio of the two spectral components for a nitroxide located in the middle of the bilayer would thus yield a water concentration in the membrane core of ~0.5 M, about 3 orders of magnitude higher than expected from theoretical estimates. In our test experiments (not shown), we did not see any appearance of a hydrogen-bonded component for nitroxides dissolved in frozen nearly saturated (~16 mM) solutions of water in toluene. Finally, a strong point in favor of considering bent conformations of *n*-PC spin labels is the non-monotonic dependence of the hydrogen-bonded fraction on n (Table 4). In a fluid membrane, the membrane depth distribution of nitroxide moieties for each spin-labeled lipid correlates to its *n*-value.[10] Higher n values show deeper average immersion, although the distribution is broad and even high n numbers show a substantial fraction of conformations with the nitroxide touching the carbonyl area. In the much denser packed gel phase, the situation can be different and the spin labels may prefer defects in the lipid structure.[53,54] One of the areas with such defects is just above the cholesterol rings, and this should correspond to a hydrophobic local environment. It can be reached by the nitroxide of 10-PC but not 7-PC. This would explain the jump in the fraction of nonpolar component between 7- and 10-PC, while further decrease in this fraction could be attributed to U-shaped conformations for higher values of n. These conformations put the nitroxide moiety back

dx.doi.org/10.1021/jp211879s | J. Phys. Chem. B 2012, 116, 6694−6706

to the surface region with high water content, while the hydrocarbon chain mostly remains located in the hydrophobic part of the membrane.

DMPC and DPPC without Cholesterol. It has been previously observed that, in the absence of cholesterol, PC spin labels in DPPC[19] and DMPC[21] under rigid limit conditions have a strong broad background signal. This signal points at aggregation of spin labels and is most pronounced for the 7−12 PC positions. Since no significant signs of such aggregation are seen in the fluid phase of the membrane or in the gel phase in the presence of cholesterol, this aggregation can be specifically attributed to the gel or crystalline (subgel) state of pure-lipid membranes. Also, since diffusion in the gel phase is slow, one can expect hysteresis effects and effects of the sample-treatment procedure; see refs 55 and 56.

Figure 6 shows spectra of PC spin labels in DMPC membranes without cholesterol. These spectra were recorded

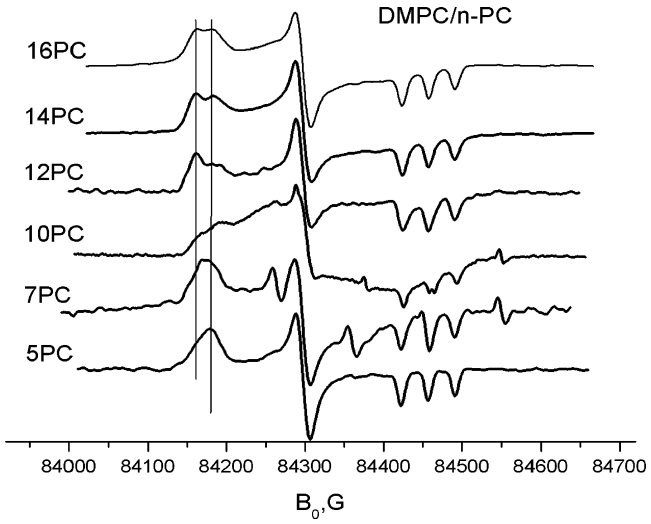

Figure 6. *n*-PC spin labels in DMPC with no cholesterol at 80−82 K. The samples are gradually frozen in the flow of gaseous nitrogen. The vertical lines indicate g values of 2.00882 and 2.009435. (The additional superposition signal for 7-PC originates from an occasional manganese impurity in the sample holder).

after the sample was slowly cooled from 295 to 85 K within ~2 h. As in the presence of cholesterol, two components with different g_{xx} are clearly discernible. However, another broad, unresolved component, which is present for all spin labels but most pronounced for 7−12 PC, follows a previously observed[19] pattern for DPPC at 250 GHz . Our 240 GHz data for DPPC obtained under the same conditions as those for DMPC are very similar to the 250 GHz results by Earle et al.[19] and shown in Figure 7. A nonpolar (non-hydrogen-bonded) component similar to the nonpolar component in membranes containing cholesterol can be identified by its characteristic g_{xx} value. However, there is an important and obvious difference between DMPC and DPPC at first inspection. In DPPC, there is only one resolved component which shows the g_{xx} value corresponding to the non-hydrogen-bonded state of the nitroxide, while in DMPC two components are clearly discernible in the spectrum. This observation is in good accord with the X-band results, which indicate a less polar environment reported by high values of n in DPPC compared to DMPC (cf. Table 1, Figure 1).

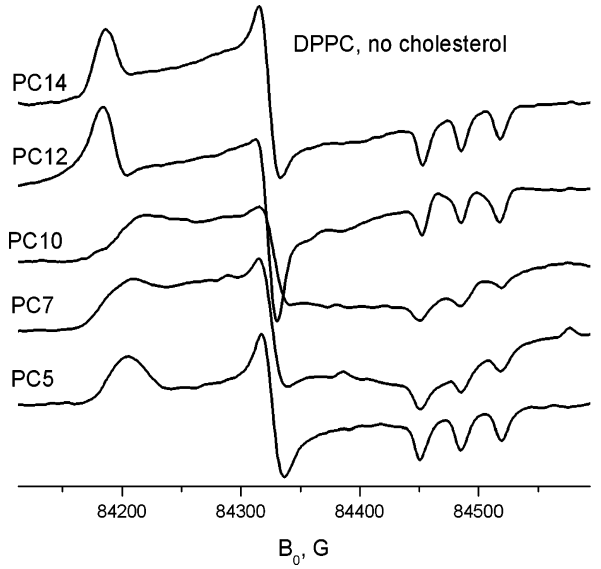

Figure 7. *n*-PC spin labels in DPPC with no cholesterol at 80−82 K. The samples are gradually frozen in the flow of gaseous nitrogen.

It is very unlikely that small structural differences between the gel phase bilayers of DMPC and DPPC[57,58] cause dramatically different water penetration into these membranes. Moreover, it has been recently shown that water penetration into the membrane depends rather on the surface area of the lipid (which is nearly identical for DMPC and DPPC) than on the membrane thickness.[59] Thus, it makes the explanation of the difference between DMPC and DPPC through dramatically different water concentration very unlikely. Even more intriguing, the average environment of the nitroxide in DPPC looks, at first glance, less polar in the absence of cholesterol, since no component with a clear peak at smaller g_{xx} can be detected, cf. Figure 8.

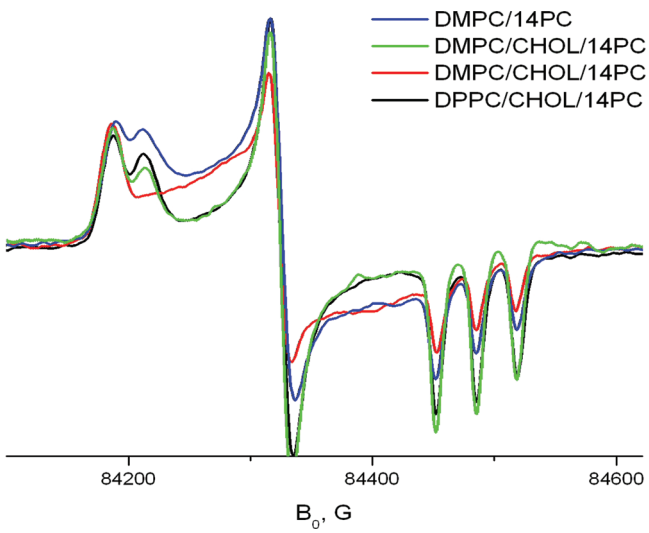

Figure 8. Comparison of 14-PC spin labels in DMPC and DPPC with/without cholesterol. All samples are slowly frozen in the flow of gaseous nitrogen. While in the presence of cholesterol the spectra can be described as a superposition of two rigid-limit components (cf. Figure 5), the most salient feature in the absence of cholesterol is a broad singlet-like background signal.

dx.doi.org/10.1021/jp211879s | J. Phys. Chem. B 2012, 116, 6694−6706

However, the most salient feature of all spectra, both DMPC and DPPC, in the absence of cholesterol, is a broad singlet-like background signal which accounts for most of the spins. The location of spins responsible for this background is unclear. In Figure 8, one can see an apparent broadening of the hydrogen-bonded component in DMPC and complete absence of this component in DPPC, concomitant with an increase in the background. A likely explanation for these observations is that the hydrogen-bonded and non-hydrogen-bonded forms of PC spin labels aggregate differently. If the hydrogen-bonded form is more prone to aggregation than the non-bonded one, it likely becomes broader due to more interactions between spins. In the superposition, spectral peaks from this broad component are less intense and eventually, with an increase in broadening, not discernible at all. To test this hypothesis, we cooled our samples very rapidly in an attempt to trap the hydrogen-bonded component before aggregation could occur.

Slow Cooling vs Quick Submerging into Liquid Nitrogen. Quantitative study of aggregation in the gel or subgel phases is difficult because of the slow diffusion rates and various hysteresis effects. For example, even though the gel phase of DPPC does not favor formation of gramicidin channels, it takes an hour to several days for these channels to dissociate.[56] There are also indications pointing to a relatively slow time scale for aggregation of PC spin labels in the gel phase. Figure 9 shows

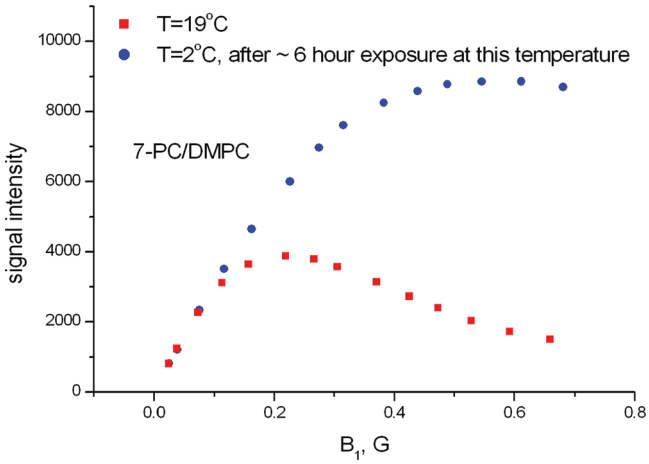

Figure 9. Change in the relaxation curve of 7-PC in DMPC under exposure at 2 °C. This increase in relaxation occurs gradually within several hours, and it can be completely reversed by a brief exposure at 19 °C.

saturation curves for 0.5 mol % of 7-PC in DMPC. At 19 °C, in the P_β phase, this system shows good saturation, with a *P* parameter of ~19. Saturation measurements performed immediately after cooling to 2 °C give a similarly high *P* value. However, after longer exposure at this temperature, the *P* value starts to decrease and after several hours drops below 2. This increase in relaxation is very likely due to aggregation, and this aggregation appears to be a relatively slow process at 2 °C. Also, this increase in relaxation is reversible; return to 19 °C reverses the aggregation and the *P* value. Although a temperature of 2 °C should correspond to the subgel phase, the exact phase state of the lipid at this condition is not obvious due to likely supercooling; see below. It usually takes days at this temperature to form the L_C phase, which then can be characterized by X-ray diffraction.

Previously, similar observations of exclusion of 5-PC spin labels from DPPC after exposure at 0 °C by using saturation transfer ESR[60] were attributed to formation of a subgel phase.

We expected that quick freezing (within ~0.2s) of the sample by instantly submerging into liquid nitrogen should substantially eliminate these slow lipid rearrangement effects compared to the standard slow cooling procedure using a flow cryostat. Indeed, spectra recorded after this simple quick-freeze procedure were different from the spectra obtained by gradual cooling in a flow of gaseous nitrogen. As seen in Figure 10A, the spectrum of 14-PC in DPPC does not have a broad singlet-like component and can be well simulated by a simple superposition of two rigid limit spectra with g_{xx} = 2.00943 and g_{xx} = 2.00882. Interestingly, most 14-PC spins are present in the form of the hydrogen-bonded component, which is greater than the nonbonded one by a 2.2:1 ratio.

As seen from Figure 11, quick freezing helps to dramatically decrease the amount of the broad background signal and yields well resolved rigid-limit spectra even when a standard cooling procedure results in nearly unresolvable, broad-feature spectra.

PC Spin Labels in Gel/Subgel Phases. A Foreign Body Looking for a Harbor. One of the possible artifacts of using molecular probes as reporters in biological and model membranes is their exclusion from the membrane interior to the membrane surface. Such exclusion of certain molecules or structural units is a natural feature of membrane biological function. For example, exclusion of tryptophans and their affinity to the membrane interface is an important factor in lipid−protein interactions and stabilization of certain conformations of transmembrane protein/peptides.[61] Exclusion from the bilayer and formation of some U-shaped conformations have been known for a long time for a number of fluorescent labels.[8,9,11]

Spin labels are usually considered as more adequate molecular probes for lipid bilayers, as evidenced by studies in fluid membranes (see the Introduction). Indeed, in the L_α phase of model membranes or natural biological membranes, ESR parameters of polarity, accessibility for paramagnetic molecules, and molecular dynamics parameters[1,3,4] reported by PC spin labels change monotonically with an increasing value of *n*. NMR also shows that, despite a relatively broad distribution of conformations, the average depth position of *n*-PC nitroxides increases with *n*.

However, our current study shows that in the gel phase the situation is very likely different. Several ESR parameters (accessibility for Ni^{2+} ions absorbed on the membrane surface, hyperfine tensor, and g-tensor components) unambiguously indicate that in the gel phase a substantial fraction of nitroxide is located in the membrane region with high water content.

An alternative explanation through water penetration into the membrane interior is unsuccessful because (1) it requires several orders of magnitude higher water content in the middle of the membrane than any known theoretical prediction and (2) it cannot explain nongradual change in the fraction of hydrogen-bonded nitroxide along the PC series. On the other hand, assuming a high statistical weight of bent conformations with the nitroxide moiety close to the membrane surface can better explain these observations. Pure lipids DMPC and DPPC form the L'_β "tilted gel" phase with densely packed and relatively well ordered hydrocarbon chains. The ability of nitroxide groups on spin-labeled stearic acids to be excluded from hydrocarbon environments and form U-shaped conformations has been previously reported.[12,13] In principle,

dx.doi.org/10.1021/jp211879s | J. Phys. Chem. B 2012, 116, 6694−6706

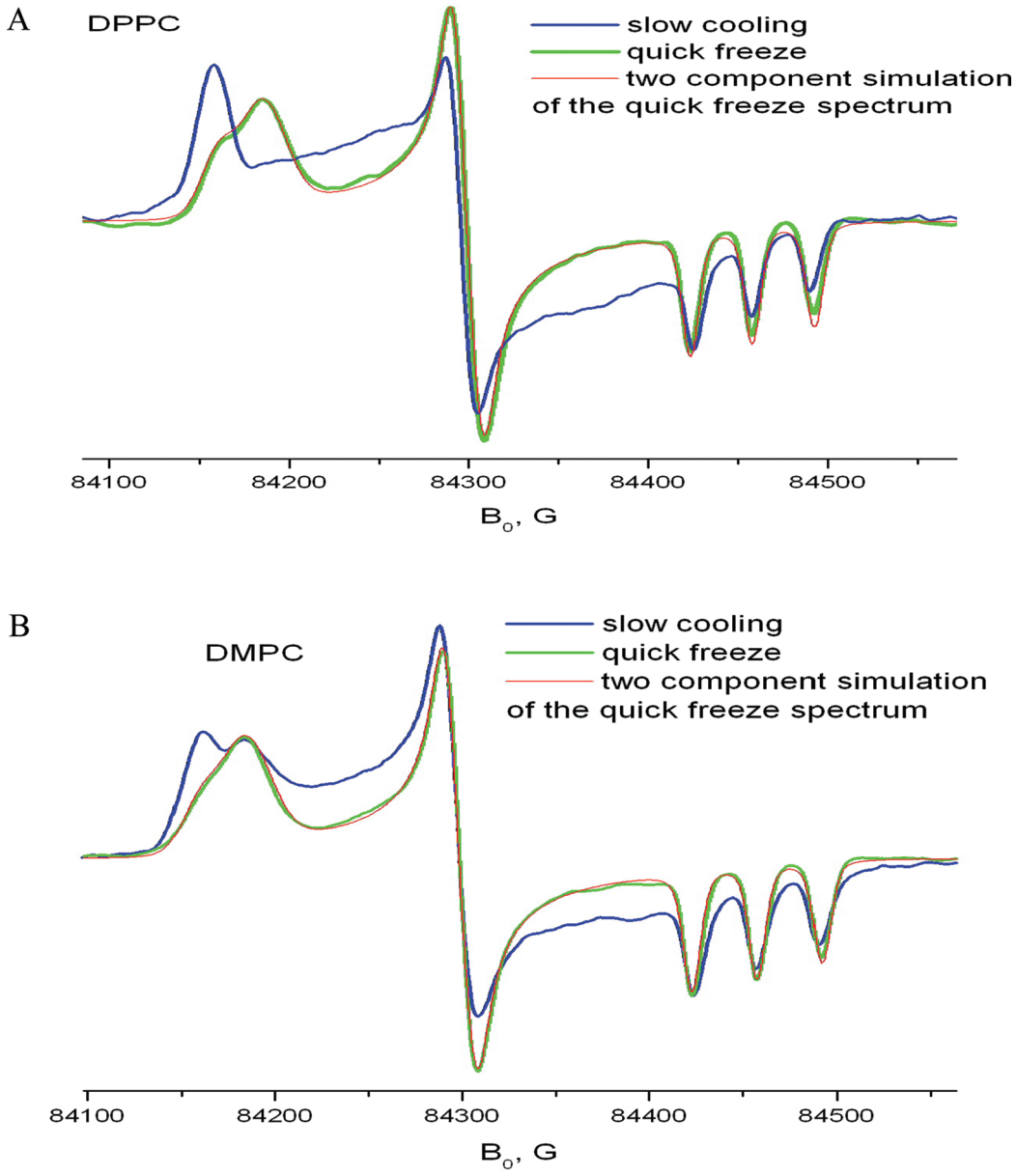

Figure 10. 14-PC in DPPC (A) and DMPC (B): gradual cooling vs quick freeze by submerging into liquid nitrogen. The spectra are recorded at 80−82 K. In the case of quick freezing, the broad unresolved component disappears and the spectrum can be well described as a superposition of HB/non-HB forms of the nitroxide. The HB/non-HB ratio is 2.2:1 for DPPC and 3.1:1 for DMPC.

formation of the L'_β phase can be compared with freezing of a bulk three-dimensional solvent. In this case, solutes are excluded from crystallizing solvent and form some regions with high local concentration. If the solute is a nitroxide radical, freezing of its solution in non-glass-forming media is well-known to yield a broad signal similar to one observed in DMPC or DPPC without cholesterol (Figures 6 and 7).

In the case of a lipid in the gel phase, the complete exclusion of spin labels into a separate phase with a high spin concentration appears to take two steps. The first one, exclusion of nitroxides from the hydrophobic area of the membrane, occurs once the lipid forms an L'_β or even a P_β phase (cf. Figure 1, Figure 2 for 19 °C, the P_β phase of DMPC, also the quick-freeze spectra in Figure 10). The second stage, which is the formation of a separate phase by these bent-conformation molecules, can be attributed to lateral aggregation in the supercooled gel, possibly at the gel/subgel phase transition.

Although formation of subgel phases was initially observed after storing a multilamellar suspension of DPPC at ∼0 °C for several days,[30] there are reports of quicker gel/subgel transformations in DPPC and DMPC. For example, in one protocol,[62] the subgel (SGII) phase in DPPC forms at about 7 °C upon cooling at 2 °C/min. These conditions are very similar to cooling conditions observed in our "slow cooling" experiment, and, in general, the cooling conditions usually existing in standard helium/nitrogen cryostats. For DMPC, formation of the subgel phase was reported after incubation at temperatures of −5 °C or lower for 2 h.[63] However, the kinetics of subgel formation is complex[64] and in some cases the final subgel phase contains spectroscopic features characteristic for the L'_β phase.[65] It could be possible that aggregation of spin labels does not require a complete transformation into the

dx.doi.org/10.1021/jp211879s | J. Phys. Chem. B 2012, 116, 6694−6706

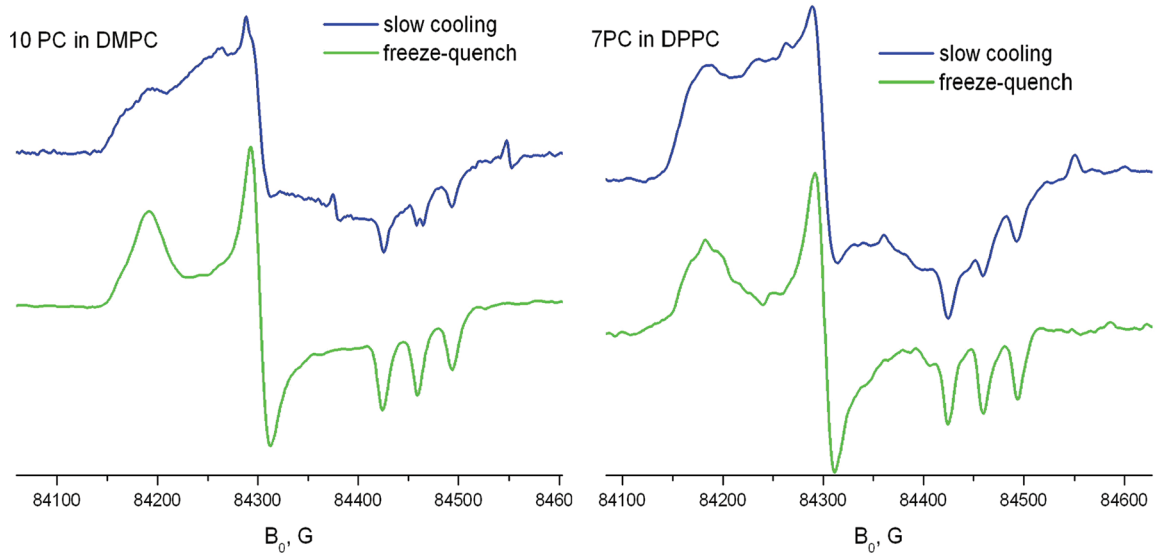

Figure 11. Obtaining better resolved spectra by quick freezing in liquid nitrogen.

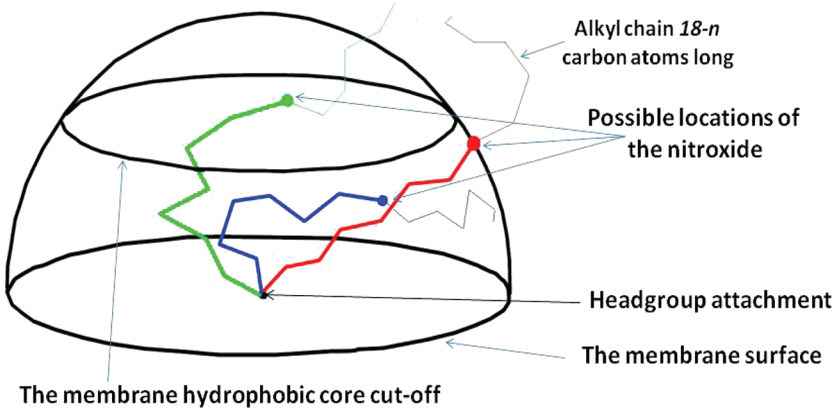

Figure 12. A model of a random distribution of conformations of the spin-label tethers for 7-PC. It puts the spin label in some random position within the half-sphere. The spherical cap is the intersection of the area available for the nitroxide and the hydrophobic core of the membrane.

subgel phase, in the sense of giving a clean X-ray pattern, and can happen sooner during cooling.

Again, we would like to stress that exclusion of nitroxides from the hydrophobic membrane core occurs in all gel phases and is a separate effect from the succeeding lateral aggregation in the supercooled gel phase.

Our quick freeze vs slow cooling experiments can also help answer an important question about the nature of the two components in the 240 GHz spectrum. Does the component with a larger g_{xx} correspond to the location of the nitroxide in the hydrophobic part of the membrane? Or both components arise from equilibrium of the hydrogen-bonded/non-hydrogen-bonded forms in the same location, like TEMPONE in ethanol (cf. Figure 3)? The different aggregation behavior of spins contributing into these components points to their different location. That is, the major hydrogen-bonded component comes from nitroxides excluded from the hydrophobic part into the area with high water content, while the minor nonpolar component may arise from spins somehow trapped in the defects of the hydrophobic membrane core.

Frozen DMPC/DPPC Membranes with Cholesterol: Partition-Like Depth Distribution of Spin Labels. As seen in Figure 5 and Table 4, in frozen membranes of both DPPC and DMPC in the presence of 30% cholesterol, all PC spin labels show well-resolved rigid limit spectra with no broad features. There is little change in the ESR line shape for quick freeze vs slow cooling in this case. Starting from 7-PC (i.e., $n \geq 7$), all spectra consist of two components. Fractions of these components approximately determined by spectral simulations are given in Table 4. Clearly, there is an abrupt jump in the fraction of non-hydrogen-bonded compound from 7- to 10-PC which is followed by a gradual decrease in this fraction with further increase in n. This observation is difficult to explain using simple models. Indeed, if we assume that the spin-labeled *sn* chain takes on mostly the fully extended conformation, we would indeed observe a similar jump after the nitroxide moiety reaches the hydrophobic core of the membrane, but with further increase in the n number, the hydrogen-bonded fraction would decrease and quickly disappear.

Another limiting case suggests that the acyl-chain hydrocarbon tether connecting the nitroxide to the lipid headgroup can take all possible coil conformations of the chain. It will put the possible position of the nitroxide of an *n*-PC spin label anywhere within a half sphere with a radius of the all-stretched conformation for the nitroxide tethers. This half sphere would rest on the membrane surface (cf. Figure 12). The ratio of hydrogen-bonded/unbonded components would be opposite to the volume ratio of the spherical cap, which is cut off by the

dx.doi.org/10.1021/jp211879s | J. Phys. Chem. B 2012, 116, 6694–6706

border of the hydrophobic core of the membrane, and the rest of the half sphere. If the cap height is half of the sphere radius, the ratio will be 2.2, similar to what we see for 7-PC (Table 5).

Table 5. Estimates for the Ratio of Hydrogen-Bonded and Non-Hydrogen-Bonded Components Based on the Simple Model Shown in Figure 12[a]

n-PC	5	7	10	12	14	16
HB/non-HB	7.2	2.2	1.01	0.74	0.58	0.48

[a]The location of the nitroxide moiety is considered in the hydrophobic core of the membrane if the distance to the membrane surface is more than half of the acyl tether for 7-PC in the fully extended conformation ("3.5-PC").

Using this observation to set (in a rather arbitrary fashion) the cutoff of the hydrophobic core at "3.5" PC, half of the acyl tether for 7-PC in the fully extended conformation, and further applying the formula for the spherical cap, we get the following predictions for the ratio of components.

Although this model is qualitatively better when compared to Table 4, it does not reproduce the observed abrupt drop between positions 7 and 10. Choosing different cutoff values or slightly modifying the model by using a cone instead of a whole half-sphere does not substantially improve it. Also, no model assuming some random distribution of nitroxide depth position would reproduce the decrease in the hydrophobic fraction with further increase in n beyond 10.

To better explain the observed effects, one could assume some set of preferential depth positions in the membrane to be occupied by the nitroxide ring. These positions may be areas of defects in the membrane structure, which can more easily accommodate a structure-disturbing nitroxide moiety than areas with compact alignment of hydrocarbon chains. One of the areas of such defects could start above the end of the rigid fused-ring system of cholesterol,[66] which is about the level reachable by *n*-PC labels starting from $n = 9$. Once the tether length is sufficient, nitroxides start populating these favorable locations, causing the change in the component ratio. However, the preference of the nitroxide ring for the location in the hydrophobic part of a DMPC/cholesterol or DPPC/cholesterol membrane does not completely overwhelm its affinity to some sites close to the membrane surface. It gives a partition-like distribution between the two sites which is observable in the spectrum of all *n*-PC labels with $n > 7$ as two components.

A gradual decrease in the hydrogen-bonded fraction between 10-PC and 16-PC can also be explained using this partition model. For an *n*-PC spin label, the same carbon atom of the nitroxide ring that is connected to the acyl tether also has a hydrocarbon tail with a length of *18-n* carbons attached. Bringing the nitroxide label of 10-PC to the membrane surface will require, on average, placing more hydrophobic CH_2 groups to the polar area than for 16-PC. This will be associated with some energy penalty preventing the nitroxide of 10-PC from leaving the hydrophobic core and affecting the partition. Note also a slight drop in the accessibility of the 10-PC position for Ni^{2+} ions for cholesterol-free DMPC membranes, which may have the same origin.

What about Biological Membranes? The gel phase rarely exists in biological membranes, and the subgel phase is unknown for them. However, polarity measurements in frozen natural membranes using PC spin labels can also be affected by the affinity of spin labels to some structural defects, especially in the presence of proteins. For example, all PC labels in mixtures of DPPC with gramicidin A show about the same g_{xx} value, indicative of the same polarity,[19] most likely due to an interaction with the peptide's α-helical structure. Also, natural membranes usually have complex lipid headgroup composition and a variety of lengths and unsaturation in acyl chains. This can affect the free volume available for spin labels both in the hydrophobic core and in the membrane interface. Figure 13 shows 240 GHz spectra for 14-PC in egg-yolk lecithin with and without cholesterol.

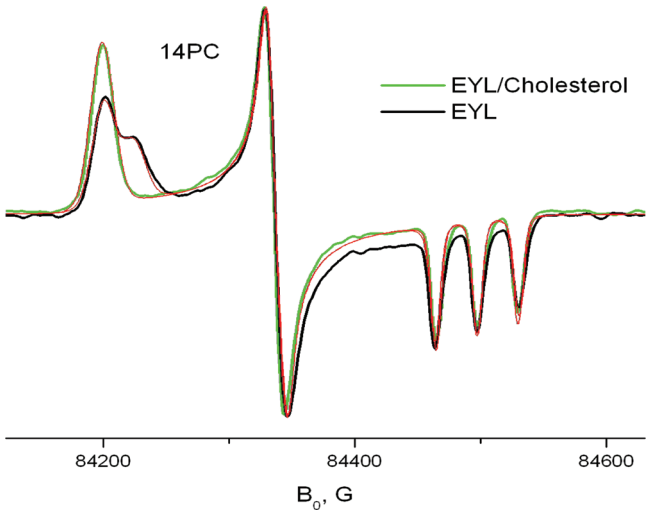

Figure 13. 14-PC in EYL with and without cholesterol at 82 K. The samples are gradually frozen in the flow of gaseous nitrogen. The corresponding one- and two-component (the ratio of components with g_{xx} = 2.009410 and 2.008820 is 0.5) rigid limit simulations are shown in red.

One can see that, similar to DMPC and DPPC membranes, the fraction of the hydrogen-bonded component drops with addition of cholesterol (cf. Figure 5 and the quick-freeze spectra in Figure 10). However, compared to DMPC and DPPC membranes, this fraction in EYL is lower. Actually, in EYL/cholesterol, only a nonpolar component can be observed in the spectrum. It can be explained by the presence of a double bond in the acyl chain of EYL. This unsaturated bond has a kink, which disrupts the packing of lipids. It creates extra free space in the hydrophobic core of the membrane,[67] and thus may shift the partition of nitroxides in favor of the membrane interior. Also, a variety of headgroups may improve packing in the polar head area, additionally forcing nitroxides into the hydrophobic core.

CONCLUSIONS

Location of the reporter nitroxide moiety in frozen membranes with and without cholesterol was studied using ESR at 9 and 240 GHz.

(1) Test experiments on four different nitroxide radicals in solvents of different polarity showed that 240 GHz ESR can clearly detect three components having three distinct g_{xx} values: (1) "non-polar", (2) "polar", (3) "very polar". In some solvents, these components coexist, for example, (1) and (2) in ethanol, (2) and (3) in water/glycerol and TFE, and can be separated as distinct peaks in the X-region of the spectrum. These three components should

dx.doi.org/10.1021/jp211879s | J. Phys. Chem. B 2012, 116, 6694–6706

be attributed to different hydrogen-bonding states of the nitroxide.

(2) In frozen lipid membranes with or without cholesterol, *n*-PC spin labels with $n > 7$ usually show two-component 240 GHz ESR spectra. These components correspond to hydrogen-bonding states (1) and (2). We attribute the hydrogen-bonded component for $n > 7$ to bent conformations of the spin-labeled molecule, with the nitroxide close to the membrane surface. In membranes without cholesterol, ESR spectra obtained by relatively slow sample cooling in the flow of gaseous nitrogen show also a broad background signal, most pronounced for PC labeling positions 7−12.

(3) Additional evidence for the presence of such bent conformations and their prevalence in the gel phase DMPC membranes without cholesterol was obtained at 9.5 GHz ESR from A_{zz} values determined at 77 K and by relaxation enhancement for PC spin labels from Ni^{2+} ions absorbed at the membrane surface at 19 °C (P_β phase).

(4) If instead of slow cooling a sample of cholesterol-free membrane of DMPC or DPPC is quickly frozen by being instantly submerged into liquid nitrogen, the broad background signal is replaced by the hydrogen-bonded component.

(5) We believe that the appearance of bent *sn-2* chain conformations due to exclusion of nitroxides from pure lipids occurs at the formation of all gel phases, including the P_β rippled phase. In a sense, this process is similar to exclusion of solutes from a crystallizing three-dimensional solvent. However, further slow formation of a separate phase of spin-labeled lipid which manifests itself in the broad background ESR signal occurs in the supercooled gel. It could be likely attributed to the effects of a gel/subgel phase transition.

(6) In membranes containing cholesterol, the observed ratio of the hydrogen-bonded components can be best described by a partition-like equilibrium between nitroxides located in defects of lipid structure in the hydrophobic core of the membrane and close to the membrane surface.

(7) The main conclusion of this work is that the ESR parameters of PC spin labels in frozen model membranes and, quite likely, in the majority of biological membranes do not follow the membrane polarity profile, water penetration profile, or any other continuously changing property of membrane environment. Instead, they reflect a distribution between hydrogen-bonded and non-hydrogen-bonded forms of the nitroxide. This distribution is affected by a number of factors in the membrane composition, chain packing in the lipid phase, and folding properties of the *sn-2* spin-labeled chain itself for each specific PC label.

■ ASSOCIATED CONTENT

Supporting Information

(1) X-band spectra of *n*-PC labels in DMPC/cholesterol, DPPC, and DPPC/cholesterol at 77 K, (2) spectra of TEMPOL, TEMPO, and 2,2,5,5-tetramethyl-3-pyrrolin-1-oxyl-3-carboxylic acid in a series of glass-forming solvents at 80−85 K, (3) estimates of the hydrogen bonding constants for nitroxides from the A_{zz} values measured at 77 K at X-band. This material is available free of charge via the Internet at http://pubs.acs.org.

■ AUTHOR INFORMATION

Corresponding Author

*Phone: (607) 255-3647. Fax: (607) 255-0595. E-mail: jhf3@cornell.edu.

Notes

The authors declare no competing financial interest.

■ ACKNOWLEDGMENTS

This work was supported by the National Institute of Health, grants NIH/NIBIB R010EB003150, NIH/NCRR P41-RR 016292, and NIH/NIGMS P41GM103521. We are grateful to Siddarth Chandrasekaran for help in some experiments.

■ LIST OF ABBREVIATIONS

HF ESR, HFHF ESR: high field ESR, high field/high frequency ESR
DMPC: 1,2-dimyristoyl-*sn*-glycero-3-phosphocholine
DPPC: 1,2-dipalmitoyl-*sn*-glycero-3-phosphocholine
EYL: egg yolk lecithin
n-PC spin labels: 1-palmitoyl-2-stearoyl-(*n*-doxyl)-*sn*-glycero-3-phosphocholines
TFE: 2,2,2-trifluoroethanol
MCH: methylcyclohexane
TEMPO: 2,2,6,6-tetramethylpiperidine-*N*-oxyl
TEMPOL, 4-hydroxy-TEMPO: 4-hydroxy-2,2,6,6-tetramethylpiperidine-*N*-oxyl
TEMPONE, oxo-TEMPO: 4-oxy-2,2,6,6-tetramethylpiperidine-*N*-oxyl

■ REFERENCES

(1) Swamy, M. J.; Ciani, L.; Ge, M.; Smith, A. K.; Holowka, D.; Baird, B.; Freed, J. H. *Biophys. J.* **2006**, *90*, 4452−4465.
(2) Altenbach, C.; Greenhalgh, D. A.; Khorana, H. G.; Hubbell, W. L. *Proc. Natl. Acad. Sci. U.S.A.* **1994**, *91*, 1667−1671.
(3) Marsh, D. *Proc. Natl. Acad. Sci. U.S.A.* **2001**, *98*, 7777−7782.
(4) Dzikovski, B.; Livshits, V. A.; Marsh, D. *Biophys. J.* **2003**, *85*, 1005−1012.
(5) Marsh, D.; Watts, A.; Pates, R. D.; Uhl, R.; Knowles, P. F.; Esmann, M. *Biophys. J.* **1982**, *37*, 265−274.
(6) Costa-Filho, A. J.; Borbat, P. P.; Crepeau, R. H.; Ge, M.; Freed, J. H. *Biophys. J.* **2003**, *84*, 3364−3378.
(7) Krishnan, K. S.; Balaram, P. *FEBS Lett.* **1975**, *60*, 419−422.
(8) Ashcroft, R. G.; Thulborn, K. R.; Smith, J. R.; Coster, H. G. L.; Sawer, W. H. *BBA* **1980**, *602*, 299−308.
(9) Chattopadhyay, A.; London, E. *Biochemistry* **1987**, *26*, 39−45.
(10) Vogel, A.; Scheidt, H. A.; Huster, D. *Biophys. J.* **2003**, *85*, 1691−1701.
(11) Cadenhead, D. A.; Keller, B. M. J.; Muller-Landau, F. *BBA* **1975**, *382*, 253−259.
(12) Dzikovski, B.; Livshits, V. *Phys. Chem. Chem. Phys.* **2003**, *5*, 5271−5278.
(13) Baglioni, P.; Dei, L.; Rivara-Minten, E.; Kevan, L. *J. Am. Chem. Soc.* **1993**, *115*, 4286−4290.
(14) Marsh, D. *Appl. Magn. Reson.* **2010**, *37*, 435−454.
(15) Ellena, J. F.; Archer, S. J.; Dominey, R. N.; Hill, B. D.; Cafiso, D. S. *BBA* **1988**, *940*, 63−70.
(16) Bouwstra, J. A.; Salomons-de Vries, M. A.; van der Speck, J. A.; Bras, W. *Int. J. Pharmacol.* **1992**, *84*, 205−216.
(17) Pilgram, G. S. K.; Engelsma-van Pelt, A. M.; Bouwstra, J. A.; Koerten, H. K. *J. Invest. Dermatol.* **1999**, *113*, 403−409.
(18) Widomska, J.; Raguz, M.; Dillon, J.; Gaillard, E. R.; Subczynski, W. K. *BBA* **2007**, *1768*, 1454−1465.
(19) Earle, K. A.; Moscicki, J. K.; Ge, M.; Budil, D. E.; Freed, J. H. *Biophys. J.* **1994**, *66*, 1213−1221.

(20) Subczynski, W. K.; Wisniewska, A.; Yin, J.-J.; Hyde, J. S.; Kusumi, A. *Biochemistry* **1994**, *33*, 7670−7681.
(21) Kurad, D.; Jeschke, G.; Marsh, D. *Biophys. J.* **2003**, *85*, 1025−1033.
(22) Smirnova, T. I.; Smirnov, A. I. High Field EPR Spectroscopy in Membrane and Protein biophysics. In *ESR spectroscopy in Membrane Biophysics*; Hemminga, M. A., Berliner, L. J., Eds.; Springer: New York, 2007; Vol. *27*.
(23) Barnes, J. P.; Freed, J. H. *Rev. Sci. Instrum.* **1997**, *68*, 2838−2846.
(24) Zhang, Z.; Fleissner, M. R.; Tipikin, D. S.; Liang, Z.; Moscicki, J. K.; Earle, K. A.; Hubbell, W. L.; Freed, J. H. *J. Phys. Chem. B* **2010**, *114*, 5503−5521.
(25) Fajer, P.; Marsh, D. *J. Magn. Reson.* **1982**, *49*, 212−224.
(26) Kooser, R. G.; Volland, W. V.; Freed, J. H. *J. Chem. Phys.* **1969**, *50*, 5243−5257.
(27) Livshits, V. A.; Dzikovski, B.; Marsh, D. *J. Magn. Reson.* **2001**, *148*, 221−237.
(28) Earle, K.; Dzikovski, B.; Hofbauer, W.; Moscicki, J. K.; Freed, J. H. *Magn. Reson. Chem.* **2005**, *43*, S256−S266.
(29) Stoll, S.; Schweiger, A. *J. Magn. Reson.* **2006**, *178*, 42−55.
(30) Chen, S. C.; Sturtevant, J. M.; Gaffney, B. J. *Proc. Natl. Acad. Sci. U.S.A.* **1980**, *77*, 5060−5063.
(31) Marsh, D.; Kurad, D.; Livshits, V. A. *Magn. Reson. Chem.* **2005**, *43*, S20−S25.
(32) Budil, D. E.; Earle, K. A.; Lynch, W. B.; Freed, J. H. Electron paramagnetic resonance at 1 mm wavelength. In *Advanced EPR: Applications in Biology and Biochemistry*; Hoff, A., Ed.; Elsevier: Amsterdam, The Netherlands, 1989; pp 307−340.
(33) Ondar, M. A.; Grinberg, O. Y.; Dubinskii, A. A.; Lebedev, Y. S. *Sov. J. Chem. Phys.* **1985**, *3*, 781−792.
(34) Kawamura, T.; Matsunami, S.; Yonezawa, T. *Bull. Chem. Soc. Jpn.* **1967**, *40*, 1111−1115.
(35) Smirnov, A. I.; Smirnova, T. I. *Appl. Magn. Reson.* **2001**, *21*, 453−467.
(36) Smirnova, T. I.; Smirnov, A. I.; Pachtchenko, S. V.; Poluektov, O. G. *J. Am. Chem. Soc.* **2007**, *129*, 3476−3477.
(37) Bordignon, E.; Brutlach, H.; Urban, L.; Hideg, K.; Savitsky, A.; Schnegg, A.; Gast, P.; Engelhard, M.; Groenen, E. J. J.; Möbius, K.; Steinhoff, H.-J. *Appl. Magn. Reson.* **2010**, *37*, 391−403.
(38) Hwang, J. S.; Mason, R. P.; Hwang, L.-P.; Freed, J. H. *J. Phys. Chem.* **1975**, *79*, 489−511.
(39) Owenius, R.; Engström, M.; Lindgren, M.; Huber, M. *J. Phys. Chem. A* **2001**, *105*, 10967−10977.
(40) Erilov, D. A.; Bartucci, R.; Guzzi, R.; Shubin, A. A.; Maryasov, A. G.; Marsh, D.; Dzuba, S. A.; Sportelli, L. *J. Phys. Chem. B* **2005**, *109*, 12003−12013.
(41) Pavone, M.; Sillanpää, A.; Cimino, P.; Crescenzi, O; Barone, V. *J. Phys. Chem. B* **2006**, *110*, 6189−16192.
(42) Plato, M.; Steinhoff, H.-J.; Wegener, C.; Törring, J. T.; Savitsky, A.; Möbius, K. *Mol. Phys.* **2002**, *100*, 3711−3721.
(43) Keutsch, F. N.; Saykally, R. J. *Proc. Natl. Acad. Sci. U.S.A.* **2001**, *98*, 10533−10540.
(44) Earle, K.; Budil, D. E.; Freed, J. H. *J. Phys. Chem.* **1993**, *97*, 13289−13297.
(45) Freed, J. H. *Annu. Rev. Phys. Chem.* **2000**, *51*, 655−689.
(46) Dzikovski, B.; Tipikin, D. S.; Livshits, V.; Earle, K. A.; Freed, J. H. *Phys. Chem. Chem. Phys.* **2009**, *11*, 6676−6688.
(47) Budil, D. E.; Earle, K.; Freed, J. H. *J. Phys. Chem.* **1993**, *97*, 1294−1303.
(48) Marsh, D. *Eur. Biophys. J.* **2002**, *31*, 559−562.
(49) Bartucci, R.; Erilov, D. A.; Guzzi, R.; Sportelli, L.; Dzuba, S. A.; Marsh, D. *Chem. Phys. Lipids* **2006**, *141*, 142−157.
(50) Berendsen, H. J. C.; Marrink, S. J. *Pure Appl. Chem.* **1993**, *65*, 2513−2520.
(51) Carruthers, A.; Melchior, D. L. *Biochemistry* **1983**, *22*, 5797−5807.
(52) Lande, M. B.; Donovan, J. M.; Zeidel, M. L. *J. Gen. Physiol.* **1995**, *106*, 67−84.
(53) Lee, A. G. *Biochemistry* **1977**, *16*, 835−841.
(54) Rubenstein, J. L.; Smith, B. A.; McConnell, H. M. *Proc. Natl. Acad. Sci. U.S.A.* **1979**, *76*, 15−18.
(55) Dzikovski, B. G.; Borbat, P. P.; Freed, J. H. *Biophys. J.* **2004**, *87*, 3504−3517.
(56) Dzikovski, B. G.; Earle, K. A.; Pachtchenko, S. V.; Freed, J. H. *J. Magn. Reson.* **2006**, *179*, 273−277.
(57) Nagle, J. F.; Tristram-Nagle, S. *Biochim. Biophys. Acta, Rev. Biomembr* **2000**, *1469*, 159−195.
(58) Tristram-Nagle, S.; Liu, Y.; Legleiter, J.; Nagle, J. F. *Biophys. J.* **2002**, *83*, 3324−3335.
(59) Mathai, J. C.; Tristram-Nagle, S.; Nagle, J. F.; Zeidel, M. L. *J. Gen. Physiol.* **2007**, *131*, 69−76.
(60) Páli, T.; Bartucci, R.; Horváth, L.; Marsh, D. *Biophys. J.* **1993**, *64*, 1781−1788.
(61) Sun, H.; Greathouse, D. V.; Andersen, O. S.; Koeppe, R. E. I. *J. Biol. Chem.* **2008**, *283*, 22233−22243.
(62) Koynova, R.; Tenchov, B. G.; Todinova, S.; Quinn, P. J. *Biophys. J.* **1995**, *68*, 2370−2375.
(63) Chang, H. H.; Bhagat, R. K.; Tran, R.; Dea, P. *J. Phys. Chem. B* **2006**, *110*, 22192−22196.
(64) Tristram-Nagle, S.; Suter, R. M.; Sun, W.-J.; Nagle, J. F. *BBA* **1994**, *1191*, 14−20.
(65) Lewis, R. N. A. H.; McElhaney, R. N. *Biophys. J.* **1992**, *61*, 63−77.
(66) Yeagle, P. L. The role of cholesterol in the biology of cells. In *The structure of biological membranes*; Yeagle, P. L., Ed.; CRC Press: Boca Raton, FL - London - New York - Washington, DC, 2005; pp 243−254.
(67) Rawicz, W.; Olbrich, K. C.; McIntosh, T. J.; Needham, D.; Evans, E. *Biophys. J.* **2000**, *79*, 328−339.
(68) *CRC Handbook of Chemistry and Physics*, 91st ed.; National Institute of Standards and Technology: Boulder, CO, 2010.